We are IntechOpen,
the world's leading publisher of
Open Access books
Built by scientists, for scientists

4,800

Open access books available

122,000

International authors and editors

135M

Downloads

Our authors are among the

154

Countries delivered to

TOP 1%

most cited scientists

12.2%

Contributors from top 500 universities

CLARIVATE ANALYTICS

BOOK CITATION INDEX

INDEXED

WEB OF SCIENCE™

Selection of our books indexed in the Book Citation Index
in Web of Science™ Core Collection (BKCI)

Interested in publishing with us?
Contact book.department@intechopen.com

Numbers displayed above are based on latest data collected.
For more information visit www.intechopen.com

Dose Reduction on Computed Tomography Angiography Using Adaptive Control Techniques

Zhijun Cai[1], Er-Wei Bai[1] and Ge Wang[2]
[1]University of Iowa
[2]Virginia Polytechnic Institute & State University
USA

1. Introduction

With the advent of multi-slice computed tomography (CT) scanner and the sophisticated CT reconstruction algorithm, CT Angiography (CTA) is increasingly used to evaluate patient with vascular diseases (Fleischmann et al., 2006; Chow & Rubin, 2002; Rubin at al., 2001). It has many advantages over the conventional catheter angiograms: 1) non-invasiveness, 2) short acquisition time, 3) multiple viewing methods, and 4) low cost. However, the radiation exposure of CT scan has become of a wide concern due to its induction to genetic, cancerous and other diseases (Brenner et al., 2001; de Gonzalez & Darby et al., 2004). According to (Mettler et al., 2000), CT scan delivers 2/3 of the total radiation dose every year in US, and this number is climbing. On June 19th, 2007, the New York Times reported that "the per-capita dose of ionizing radiation from clinical imaging exams in the U.S. increased almost 600% from 1980 to 2006". Brenner (Brenner et al., 2001) reported that diagnostic X-rays, indicating that radiation from medical and dental scans, cause about 700 cases of cancer per year in Britain and more than 5,600 cases in US. To that end, every effort to reduce the radiation dose is appreciated and the well-known ALARA (As Low As Reasonably Achievable) principle is widely accepted in the medical community.

There are many studies have been reported on dose reduction for CT scan. Wintersperger and his colleagues (Wintersperger et al., 2000) used lower kilo-voltage and claimed the resultant image had similar sensitivity and accuracy. In Fraioli's studies (Fraioli et al., 2006), lower tube currents were used and the resultant image quality was claimed to be good enough for diagnosis. Generally, dose reduction is contrary to the image quality. In other words, reducing the radiation dose will sacrifice the image quality. However, with the advanced CT reconstruction algorithm (Yan et al., 2008; Zeng et al., 2007; Liu et al., 2009; Yin et al., 2009) and post-processing techniques (Salmon et al., 2009; Benitez et al., 2009; Zeng et al., 2008; Zhang et al., 2008), the resultant images could be held to certain diagnosis level while the radiation dose is reduced lot. Recently, control technique is found very useful in CT. It can be applied to improve the CT image quality (Lu et al., 2008; H. Bai et al., 2008), and to reduce the radiation dose reduction, for example, Automatic Exposure Control (AEC) program, which modulates the tube current to maintain the same x-ray attenuation level according to the scan angle/position of the human body.

In this chapter, we present a radiation dose reduction approach using adaptive control techniques. It is specifically for CTA scan and is based on the adaptive bolus chasing techniques. The adaptive bolus chasing techniques are capable of tracking the contrast bolus peak during the CTA scan, and ensure every segment of the blood vessel to be scanned with the possible highest bolus density. To that end, it is very likely that segment of vasculature is scanned with a much higher Contrast to Noise Ratio (CNR), which is better than enough for diagnosing. With the ALARA principle, it is straightforward to modulate the tube current and/or vary the table increment to reduce the radiation dose while keeping the resultant CT images at the same diagnosis level.

2. Method

Adaptive bolus chasing techniques, the basis of the proposed dose reduction approach, will be introduced first. After that, we will show how to estimate the radiation exposure during a CTA scan followed by the introduction of the proposed scan scheme to reduce the radiation exposure.

2.1 Adaptive bolus chasing CTA

The proposed dose reduction approach is made possible by the adaptive bolus chasing CTA techniques, which will be briefly introduced in this subsection. More details can be found in (E.W. Bai et al., 2007).

In a CTA scan, the contrast bolus is used to enhance the vasculature so that it can be distinguished from the surrounding soft tissue, which has similar physical property of the vasculature (Tublin et al., 1999; Sheafor et al., 1998). During the CTA san, it is desirable to synchronize the contrast peak and CT imaging aperture, in such a way, the CNR is maximized and the vascular diseases on resultant CT images are better shown. However, the current scan method uses a pre-set constant speed to move the CT table, which is problematic due to the complicated bolus dynamics influenced by many factors such as, patient characteristics, injection patterns, and vascular diseases (Cademartiri et al., 2002). The contrast bolus rarely flows constantly along the blood vessels. Therefore, the current constant-speed method either needs a large amount of contrast volume or results in lower CNR vascular images due to the unmatched the longitudinal position of the bolus peak and CT imaging aperture.

The adaptive bolus chasing techniques are illustrated in Fig. 1. The patient is feeding into the CT gantry at the speed of the CT table. The real-time CT images are reconstructed and meanwhile the intravascular bolus density information is extracted and fed into the adaptive bolus chasing controller. The controller uses the past and current bolus density information and the knowledge of the bolus dynamics to predict the bolus peak time for the next position and sends the signal to the table driver to vary the CT table speed accordingly. Thus, the synchronization of the bolus peak and CT imaging aperture will be realized.

2.2 Radiation dose calculation in CT scan

Generally, the effective radiation dose is affected by the tube voltage, collimator width, tube current, scanning time, and scan volume (Kalender, 2005). The following procedure is used to estimate the effective radiation dose for a CT scan.
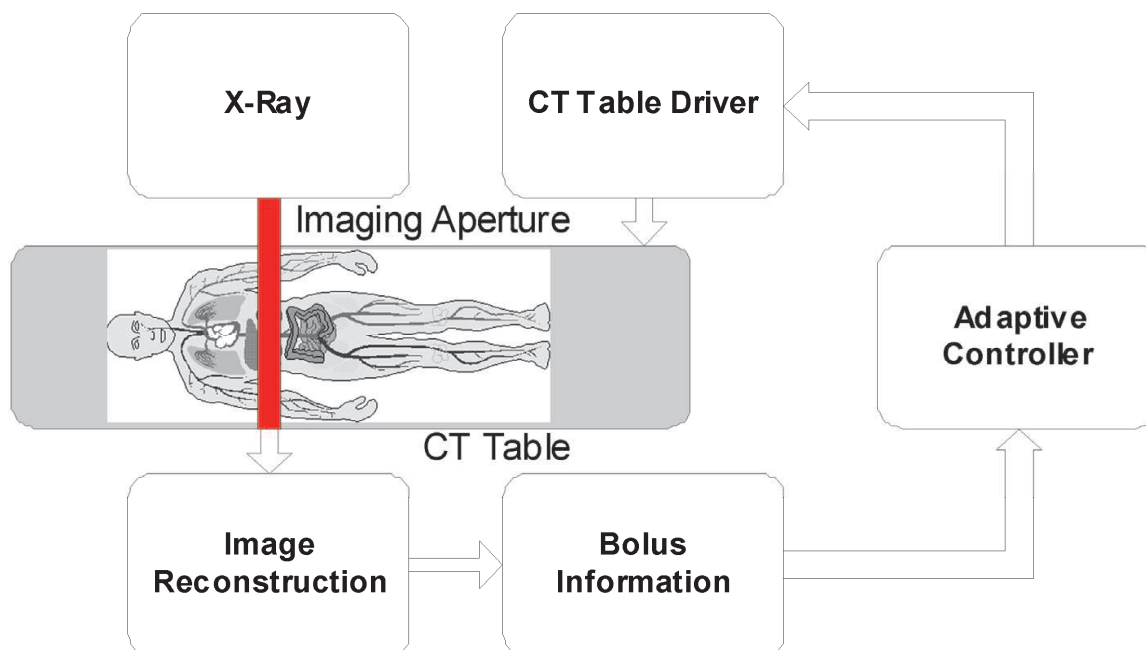
Fig. 1. Illustration of control scheme for adaptive bolus chasing CTA

1. Find the normalized weighted CT dose index (CTDI) at a specified voltage, which is given by

$$_n\text{CTDI}_w = \left(\frac{1}{3}\text{CTDI}_{100,c} + \frac{2}{3}\text{CTDI}_{100,p} \right) \tag{1}$$

where $_n\text{CTDI}_w$ denotes the normalized CTDI at 100 mAs (product of tube current and gantry rotation time), and $\text{CTDI}_{100,c}$ and $\text{CTDI}_{100,p}$ represent the measurement of phantom center and the average measurement at four different locations around the periphery of the phantom, respectively. For instance, $\text{CTDI}_{100,c}$ and $\text{CTDI}_{100,p}$ are 4.6 and 9.7, respectively, for Siemens Volume Zoom CT scanner with 120kV.

2. Compute the CTDI_{vol}. Most CTA scans are spiral scan, and adaptive bolus chasing techniques are only applicable to spiral scan; therefore, we need to compute the CTDI_{vol} for spiral scan.

$$\text{CTDI}_{vol} =_n \text{CTDI}_w \frac{W}{T} I T_r \tag{2}$$

where CTDI_{vol}, W, T, I and Tr denote CTDI volume, collimator width, tube current and gantry rotation time, respectively. W/T is called pitch in CT scan, and product of I and T_r is the effective tube current.

3. Calculate the dose length product (DLP), which is formulated as

$$DLP = \text{CTDI}_{vol} \times L \tag{3}$$

where L is the total scan length.

4. Convert the absorbed dose to effective radiation dose E

$$E = E_{DLP} \times DLP \tag{4}$$

where E_{DLP} is the region-specific conversion factor, and it equals to 0.015 for abdomen and pelvis (Shrimpton, 2009).

The above calculation is based on the constant-pitch (speed), which is not the case for the adaptive bolus chasing CTA scan. In the adaptive bolus chasing CTA scan, the CT table speed varies according to the bolus movement in the patient's vasculature. To that end, we need to modify the formula accordingly. In step 2), CTDI$_{vol}$ is computed at every step (gantry rotation time) under assumption that gantry rotation time is kept constant

$$\text{CDTI}_{vol,i} = \,_n\text{CDTI}_w \frac{W_i}{T_i} I_i T_r \tag{5}$$

Accordingly, the DLP is changed to

$$DLP = \sum_{i=1}^{N} \text{CDTI}_{vol,i} T_i = \sum_{i=1}^{N} \underbrace{\,_n\text{CDTI}_w T_r}_{C_D} W_i I_i \tag{6}$$

where T_i is the table increment at each step and N is total number of gantry rotation.

Remark

It seems that T_i is not related to DLP in Eq. (6); however, T_i affects the total number of gantry rotation. Higher average T_i results in smaller N. With all other parameters kept constant, total DLP is smaller.

2.3 Dose reduction approach using adaptive bolus chasing CTA techniques

Dose reduction can be achieved under the condition that the resultant CT images are good enough for diagnosis, which is subjective. Different physicians may have different diagnosis results for the same set of CT images. On the other hand, CT image quality is affected by many factors, such as, image noise, signal to noise ratio, antifacts and resolution. It is hard to find a standard that quantifies the image quality. Here, we focus on the CNR or Signal to Noise Ratio (SNR). Meanwhile, we restrict the spatial resolution (slice thickness) within some range.

The idea of the dose reduction approach is as follows. Since the proposed bolus chasing CTA techniques are capable of tracking the contrast bolus peak, and the scanned blood vessels are well enhanced, according to the literature, most of the segments have CT number greater than 250 HU. On the other hand, "the minimum adequate goal for contrast opcification of arterial system is 150 -200 HU" (Rubin & Rofsky, 2008). Therefore, we can modulate the tube current (and the collimator width) to achieve the desired CNR and reduce the radiation dose meanwhile.

2.3.1 Modulating the tube current

In this subsection, we propose a radiation dose reduction approach only through modulating the tube current to maintain the minimum CNR to certain level at each step. Varying the tube current and collimator width simultaneously will be presented in the next subsection.

Since we only modulate the tube current and the collimator width is kept constant, the image noise and CT number of blood vessel at step i is denoted by $\sigma_i = C_\sigma / \sqrt{I_i}$ and C_i, respectively, then the CNR at step i is $CNR_i = \sqrt{I_i} C_i / C_\sigma$ under assumption that the CT

number of the surrounding tissue is zero (or a constant value). In the adaptive bolus chasing techniques (E.W. Bai et al., 2007), we use a two-variate 2nd order polynomial to approximate the bolus density function,

$$B_i(z,t) = a_0(z_i,t_i) + a_1(z_i,t_i)t + a_2(z_i,t_i)z + a_3(z_i,t_i)t^2 + a_4(z_i,t_i)tz + a_5(z_i,t_i)z^2 \qquad (7)$$

where t and z represent the time and distant starting at the current time and position, respectively. Substitute $t = T_r = \Delta t$ and replace z with T_i (table increment at the step i), then we have

$$CNR_i = C_c \sqrt{I_i} \left(\bar{a}_0 + \bar{a}_1 T_i + \bar{a}_2 T_i^2 \right) \qquad (8)$$

where $\bar{a}_0 = a_0(t_i,z_i) + a_1(t_i,z_i)\Delta t + a_3(t_i,z_i)\Delta t^2$, $\bar{a}_1 = a_2(t_i,z_i) + a_4(t_i,z_i)\Delta t$, and $\bar{a}_2 = a_5(t_i,z_i)$.

Now, we can formulate the problem as follows:

Minimize the radiation dose (*DLP*) normalized over the table increment at every step, $C_D I_i / T_i$, under condition that CNR is kept constant or above a designated value, that is $C_c \sqrt{I_i} \left(\bar{a}_0 + \bar{a}_1 T_i + \bar{a}_2 T_i^2 \right) \geq CNR_0$, and the longitudinal resolution is not worsen very much, which is quantified by the slice thickness. The optimal solution will be given when $C_c \sqrt{I_i} \left(\bar{a}_0 + \bar{a}_1 T_i + \bar{a}_2 T_i^2 \right) = CNR_0$.

Lagrange multiplier is used to solve this problem

$$J = C_D \frac{I_i}{T_i} + \lambda \left[C_c \sqrt{I_i} \left(\bar{a}_0 + \bar{a}_1 T_i + \bar{a}_2 T_i^2 \right) - CNR_0 \right] \qquad (9)$$

The solution of the above problem is

$$T_i = \frac{-3\bar{a}_1 - \sqrt{9\bar{a}_1^2 - 20\bar{a}_0\bar{a}_2}}{10\bar{a}_2} \qquad (10)$$

and the corresponding estimated bolus density at T_i is

$$\hat{B}_i = \bar{a}_0 + \bar{a}_1 T_i + \bar{a}_2 T_i^2 \qquad (11)$$

Remark

Generally, the bolus density profile is bell-shaped (Cademartiri, 2002), to that end, $\bar{a}_2$ is negative, and $\bar{a}_1$ and $\bar{a}_0$ are positive. Without the dose reduction optimization, $T_0 = -\bar{a}_1 / (2\bar{a}_2)$ maximizes the bolus density at the next step. However, in the dose reduction approach, table increment

$$T_i = \frac{-3\bar{a}_1 - \sqrt{9\bar{a}_1^2 - 20\bar{a}_0\bar{a}_2}}{10\bar{a}_2} > \frac{-3\bar{a}_1}{5\bar{a}_2} > \frac{-\bar{a}_1}{2\bar{a}_2} > T_0$$

It is reasonable because table increment is expected to be maximized under the condition the next scan affords enough *CNR*.

Adaptive bolus chasing with dose optimization procedure through modulating tube current only

1. Identify the local bolus model, a two-variate 2nd order polynomial online as in Eq. (7). See details in (E.W. Bai et al., 2007)
2. Substitute the Δt in Eq. (7) to obtain $\bar{a}_0$, $\bar{a}_1$, and $\bar{a}_2$
3. Use Eq. (10) to compute T_i
4. Modulate tube current using $I_i = \left(B_0 / \hat{B}_i\right)^2 I_0$
5. Translate the CT table for distance T_i in time Δt
6. Until the preset length is scanned.

Remark

This algorithm alone does not guarantee that the whole vasculature length be scanned. However, by setting the minimum moving distance at each step, it is no longer a problem. This is reasonable because scanning the vasculature forever contradicts minimizing the radiation dose.

2.3.2 Modulating the tube current and collimator width

Adaptive-chasing method varies the table increment T_i at each step, and changes the pitch p accordingly, since $p = T_i/W$, where W is the collimator width. Under condition that the collimator width is constant, the slice thickness, which depends on the collimator width and table increment (see (2)), also varies. This is not good to the image quality in the sense that the longitudinal spatial resolution is not uniform. To that end, we propose to modulate the tube current and collimator width simultaneously to reduce the radiation dose and maintain the slice thickness constant.

Assume uniform slice thickness, S_0, is expected for the whole scan. For a single slice CT and half-scan reconstruction method, the slice thickness is given by

$$S_0 = \sqrt{\frac{W^2}{12} + \frac{T^2}{24}} \tag{13}$$

see (Wang & Vannier, 1984).

To keep slice thickness constant, we need to vary the collimator width at each step

$$W_i = \sqrt{12 S_0^2 - \frac{T_i^2}{2}} \tag{14}$$

Adaptive bolus chasing with dose optimization procedure through modulating tube current and collimator width

1. Identify the local bolus model, a two-variate 2nd order polynomial online as in Eq. (7)). See details in (E.W. Bai et al., 2007)
2. Substitute the Δt in Eq. (7) to have have $\bar{a}_0$, $\bar{a}_1$, and $\bar{a}_2$
3. Use Eq. (10) to obtain T_i
4. Use Eq. (14) to obtain W_i
5. Modulate tube current using $I_i = \left(B_0 / \hat{B}_i\right)^2 I_0 W_0 / W_i$
6. Translate the CT table for distance T_i in time Δt
7. Until the preset length is scanned.

3. Results

We applied the proposed dose reduction approach on the referenced digital subtraction angiogram (DSA) data sets of four patients, among which, two had occlusive diseases; one had abdominal aneurysm and one was normal. To show the advantage of the proposed method, we compared the conventional constant-speed method on the same referenced data sets. The high frame DSA data sets were collected in University of Iowa Hospital and Clinic (UIHC). They recorded the bolus information in the abdominal-aorta to the femoral artery from the time of bolus injection to the end. We extracted the bolus information along the blood vessel from every frame and formed the bolus 3D profile (position-time-density), which would be used as the referenced bolus information. It is known that the CTA data sets do not have this ability due to its narrow FOV in the longitudinal direction short acquisition time.

The CTA scan is assumed to be performed on the Siemens SOMATON Volume Zoom four-row detector CT scanner, and spiral scan mode is used. The peak Kilo-Voltage is set to 120 kV for both adaptive-chasing and constant-speed method. As for constant-speed method, we set the effective tube-current and collimator width to be 240 mAs and 10 mm, respectively. The resultant CNR of the vasculature is expected to be greater than or equal to 200 HU over the noise level generated by the above voltage, current and collimator settings.

During the simulation, the constant speed is set as 30mm/sec for all four cases. For adaptive-chasing method, the collimator width is fixed at 10mm and the pitch varies between 0.5 and 2, which also limited the CT table speed. As for the case of varying collimator width, the scanned HU results will be same. The difference is on the reconstructed CT image, and it is not discussed in this Chapter. Both methods use auto-trigged technique to start the CT table, i.e., monitor the HU in the designated region of interest (ROI), and starts the CT table when the HU reaches the pre set threshold.

The effective radiation doses for four patients are estimated in the way aforementioned in Section 2.2. To show the performance of the adaptive-chasing method and the constant-speed method, we use the performance index (PI), which is defined as

$$PI = \frac{\sum_{k=1}^{N} \hat{B}\left(z_k, \hat{t}_k\right)}{\sum_{k=1}^{N} B\left(z_k, t_k\right)} \tag{15}$$

where $B\left(z_k, t_k\right)$ is the actual maximum density at position z_k, which happens at time t_k, and $\hat{B}\left(z_k, \hat{t}_k\right)$ is the observed density at position z_k, scanned at time $\hat{t}_k$. The higher the PI, the better the performance is. However, due to the limitation on the CT table velocity and acceleration, PI is less than 1.

Fig. 2 to Fig. 5 show the patient vascular diseases and corresponding simulated scan results (CT number of the vasculature) of the adaptive-chasing and constant-speed method results. In most of the time, the scanned CT number of adaptive-chasing method (dash-dot curve) is greater than that of the constant-speed method (dashed curve).

Table 1 shows the estimated effective dose and PI for adaptive-chasing and constant-speed method, respectively. We can see that adaptive-chasing method reduces the effective dose, on average, 39% of the constant-speed method, and PI increases about 17%.
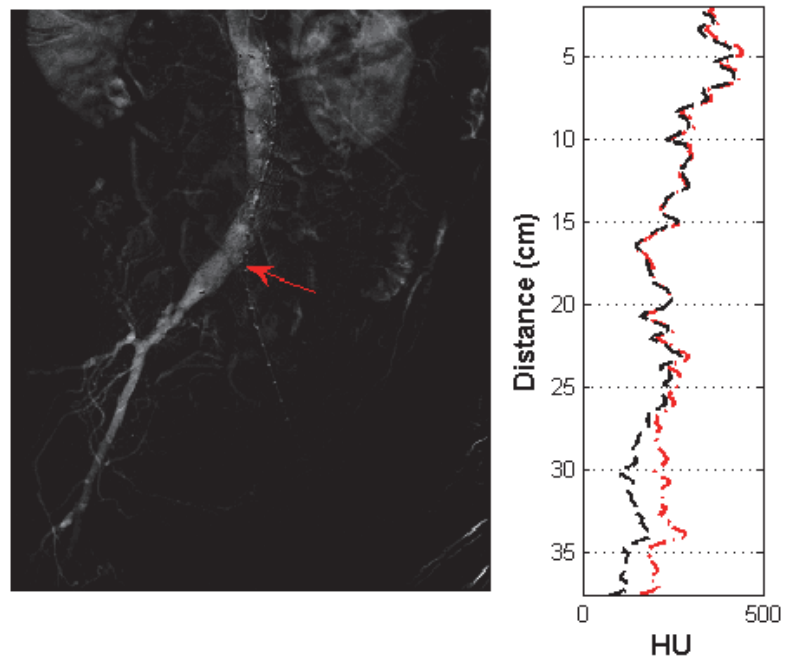
Fig. 2. The left plot is one of the DSA angiogram. It shows the occlusive vascular disease. The right plot shows the scan results of the adaptive-chasing method (dash-dot) and the constant-speed method (dashed).
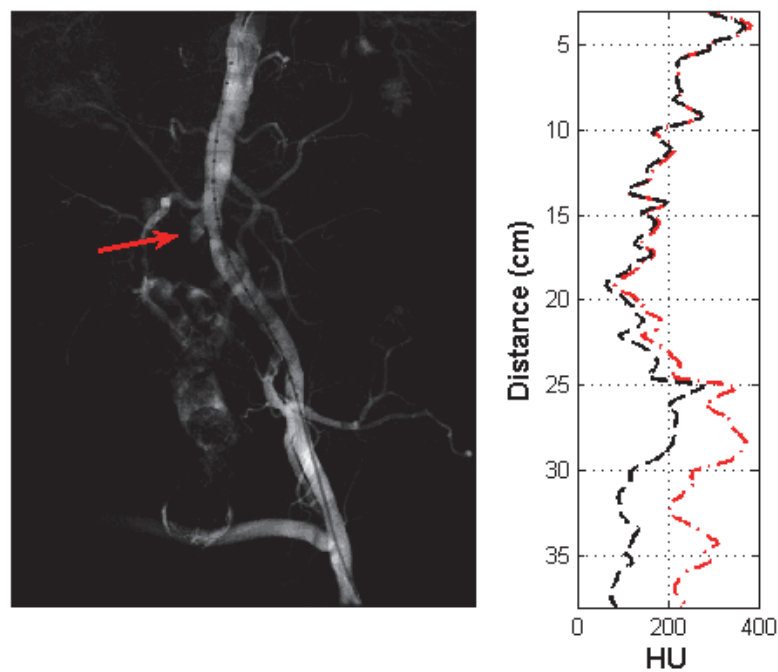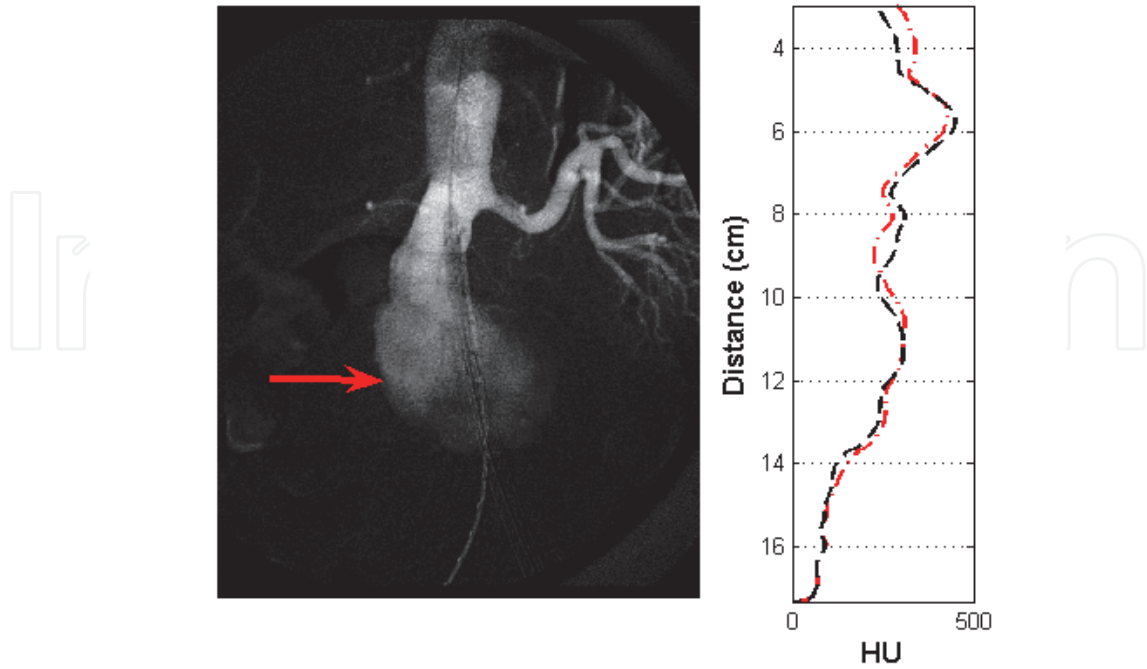

Fig. 3. The left plot is one of the DSA angiogram. It shows the occlusive vascular disease. The right plot shows the scan results of the adaptive-chasing method (dash-dot) and the constant-speed method (dashed).

Fig. 4. The left plot is one of the DSA angiogram. It shows the abdominal aneurysm disease. The right plot shows the scan results of the adaptive-chasing method (dash-dot) and the constant-speed method (dashed).
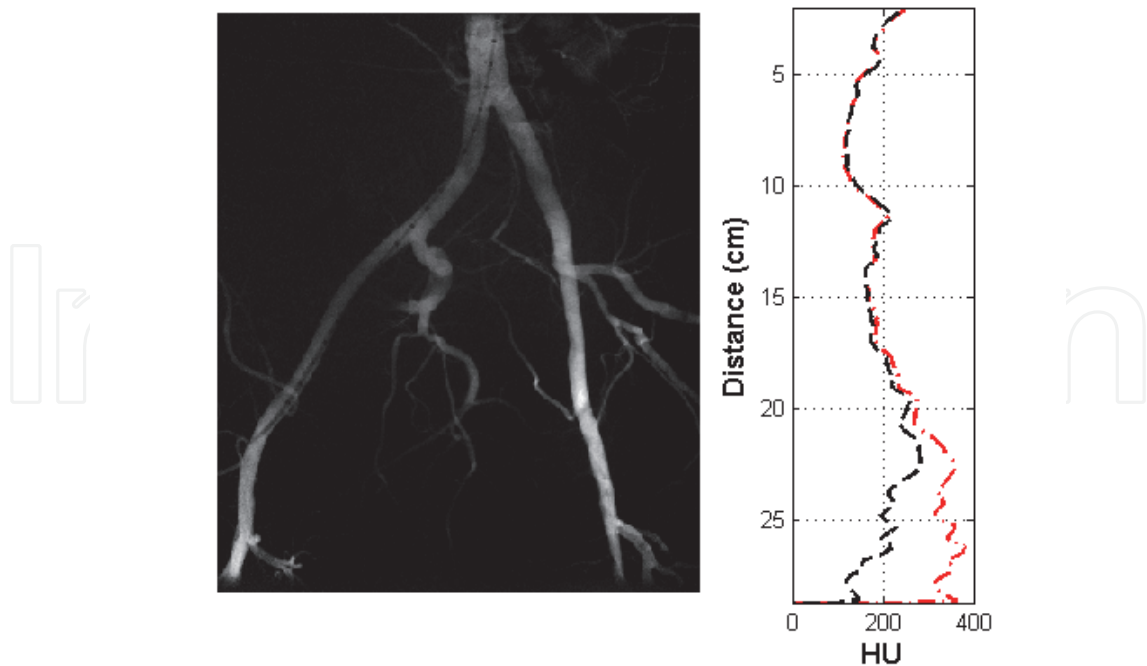

Fig. 5. The left plot is one of the DSA angiogram. No evident vascular disease is shown. The right plot shows the scan results of the adaptive-chasing method (dash-dot) and the constant-speed method (dashed).

Patient	Disease	Adaptive-Chasing method		Constant-Speed method	
		EED (msv)	PI	*EED* (msv)	PI
Patient 1	occlusive	4.95	0.97	10.73	0.84
Patient 2	occlusive	6.22	0.97	10.94	0.70
Patient 3	aneurysm	3.52	0.89	4.95	0.89
Patient 4	normal	6.57	0.96	8.25	0.79
Average		5.32	0.95	8.72	0.81

* *EED*: Estimated effective dose

Table 1. Estimated effective dose and PI for the adaptive-chasing method and constant-speed method, respectively.

4. Discussion and conclusions

The adaptive bolus chasing CTA with dose reduction is a new concept in dose reduction. It saves the radiation dose in two ways: 1) generally lowering the tube current, which is made possible through adaptive-chasing method. Though the adaptive-chasing method does not guarantee the scanned HU is greater than the expected, it generally has greater performance than the constant-speed method, which is validated in our simulations, and 2) tracking the bolus peak trajectory. The adaptive-chasing method allows the CT table to move fast when it is necessary under the condition to maintain the CNR for the scanned vasculature As we know, the faster the scan the lower radiation dose if all other parameters are kept the same.

Although the simulation is performed on a four-row detector CT scanner, this dose reduction approach could be easily extended to the 16- or 64-row detector CT scanners. Generally, 16 or 64 slice CT scanner has a wider field of view (in z direction) and moves faster. It provides much more information in a shorter time. On one hand, it is good to the control algorithm because more bolus information will make the chasing results better; on the other hand, it requires more computation capacity and challenges the real time control. This problem could be solved in following ways: 1) fast reconstruction algorithm with the advanced CPU techniques, 2) part reconstruction, which only reconstruct the images that around the region of interest. Those images are only used for real time control and the high quality CT images will be reconstructed after the scan.

The constant-speed method is not so bad for this short injection. This is because we choose a relatively good pre-set threshold to start the CT table. It is hard to set the right threshold, but a lot of contrast dose would be used to compensate for the deficit of the constant-speed method. On the other hand, adaptive-chasing method is not sensitive to the pre-set threshold. It can adjust optimal starting time by itself.

Patient 3 has an aneurysm in the abdominal aorta. When the contrast bolus flows there, it stays inside for a while until it fills the aneurysm. It is like the prolonged maximum geometry. Hence, the constant-speed method has almost the same PI as adaptive-chasing method does. However, the adaptive-chasing method saves the radiation dose by lowering the tube current while the constant-speed method does not.

We did not apply uniform slice thickness method in the simulation because it would not change the table increment, product of the tube current and collimator width, and dose savage. The only difference is the varying collimator width. We will try this method for the experiment on the CT scanner and evaluate the resultant CT image quality.

In a summary, we have proposed an adaptive-chasing method with dose reduction. The proposed approach ensures the vasculature to be scanned with higher bolus density and maintains a minimum CNR. The effective radiation dose is reduced through modulating the tube current and using the possible minimum time to track the contrast bolus. Simulation results show that the adaptive-chasing method has greater PI than the constant-speed method (0.95 vs. 0.81) and the effective radiation dose is reduced 39% on average. The proposed techniques also have great potential in optimization of contrast agent, which may save the exam cost and benefit patient who has kidney diseases. To that end, the future work will be focused on two areas: 1) the real experiment and evaluation on the resultant CT images, and 2) optimization of contrast agent.

5. References

Bai, E.W.; Cai, Z., MCcabe, R. & Wang, G. (2008). An Adaptive Optimal Control Design for a Bolus Chasing Computed Tomography Angiography. *IEEE Transactions on Control Systems Technology*, Vol. 16, pp. 60-69, ISSN: 1063-6536.

Bai, H.; Zeng, K., Bai, E. W. & Wang, G. (2008). Manual control of patient table for bolus-chasing CT angiography, *Journal of X-Ray Science and Technology*, Vol. 16, pp. 23-31, ISSN 0895-3996

Benítez, R.B.; Ning, R., Conover, D. & Liu, S. (2009). NPS characterization and evaluation of a cone beam CT breast imaging system, *Journal of X-Ray Science and Technology*, 17, pp. 17-40, ISSN 0895-3996

Brenner, D.J.; Elliston, C.D., Hall, E.J. & Berdon, W.E. (2001). Estimated risks of radiation-induced fatal cancer from pediatric CT. *American Journal of Roentgenology*, Vol. 176(2), pp. 289-296, ISSN 0361–803X

Cademartiri, F., van der Lugt, A., Luccichenti, G. & Krestin G.P. (2002). Parameters affecting bolus geometry in CTA: a review. *J Comput Assist Tomogr*, Vol. 26(4), pp. 598-607, ISSN: 0363-8715

Chow, L.C. & Rubin, G.D. (2002). CT angiography of the arterial system, *Radiol Clin North Am*, Vol. 40(4), pp. 729-49, ISSN 0033-8389

de Gonzalez, A. B. & Darby, S. (2004). Risk of cancer from diagnostic X-rays: estimates for the UK and 14 other countries. *Lancet*, Vol. 363(9406), pp. 345-351, ISSN 0140-6736

Fleischmann, D.; Hallett, R.L. & Rubin, G.D. (2006). CT angiography of peripheral arterial disease, *J Vasc Interv Radiol*, Vol. 17(1), pp. 3-26, ISSN 1051-0443

Fraioli, F.; Catalano, C., Napoli, A., Francone, M., Venditti, F., Danti, M., Pediconi, F. and Passariello, R. (2006). Low-dose multidetector-row CT angiography of the infra-renal aorta and lower extremity vessels: image quality and diagnostic accuracy in comparison with standard DSA, *Eur Radiol*, Vol. 16: 137–146, ISSN: 0938-7994

Kalender, Willi A. (2005) Computed Tomography, Fundamentals, system Technology, image quality applications, publicis MCD Verlag, ISBN: 978-3-89578-081-2

Liu, T. & Xu, J. (2009). Differential reconstruction for planar object in computed tomography, *Journal of X-Ray Science and Technology*, Vol. 17, pp. 101-114, ISSN 0895-3996

Mettler, F.A. Jr.; Wiest, P.W., Locken, J.A., & Kelsey, C.A. (2000). CT scanning: Patterns of use and dose. *Journal of Radiological Protection*, Vol. 20(4), pp. 353-359, ISSN 1361-6498

Rubin G.D. & Rofsky, N.M. (2008), CT and MR Angiography: Comprehensive Vascular Assessment, Lippinocott Williams & Wilkins, ISBN 978-0-7817-4524-3, Philadelphia

Rubin, G.D.; Schmidt, A.J., Logan, L. J., Sofilos, M. C. (2001). Multi-detector row CT angiography of lower extremity arterial inflow and runoff: initial experience, *Radiology*, Vol. 221(1), pp. 146-58, ISSN 0033-8419

Salmon, P.L.; Liu, X. & Sasov, A. (2009). A post-scan method for correcting artefacts of slow geometry changes during micro-tomographic scans, *Journal of X-Ray Science and Technology*, Vol. 17, pp. 161-174, ISSN 0895-3996

Sheafor, D.H.; Keogan, M. T., DeLong, D.M. & Nelson, R.C. (1998). Dynamic helical CT of the abdomen: prospective comparison of pre- and postprandial contrast enhancement. *Radiology*, Vol. 206(2), pp. 359-63, ISSN 0033-8419

Shrimpton P.C. (2009). Assessment of patient dose in CT: appendix C—European guidelines for multislice computed tomography. *European Commission project MSCT: CT safety & efficacy–a broad perspective Web site*.
http://www.msct.eu/PDF_FILES/EC%20CA%20Report%20D5%20-%20Dosimetry.pdf. Published March 2004. Accessed May 28, ISSN 1527- 1315

Tublin, M.E.; Tessler, F.N., Cheng, S. L., Peters, T. L., & McGovern, P. C. (1999). Effect of injection rate of contrast medium on pancreatic and hepatic helical CT. *Radiology*, Vol. 210(1), pp. 97-101, ISSN 0033-8419

Wang, G. & Vannier, M.M. (1984). Logitudinal resolution in volumetric x-ray computerized tomography-Analytical comparison between conventional and helical computerized tomography, *Med. Phys.* Vol. 21(3), pp. 429-433, ISSN: 0094-2405

Wintersperger, B.; Jakobs, T., Herzog, P., Schaller, S., Nikolaou, K., Suess, C., Weber, C., Reiser, M. & Becker, C. (2005). Aorto-iliac multidetector-row CT angiography with low kV settings: improved vessel enhancement and simultaneous reduction of radiation dose, *Eur Radiol*, Vol. 15, pp. 334–341, ISSN: 0938-7994

Yan, G.; Tian, J., Zhu, S. Dai, Y. & Qin, C. (2008). Fast cone-beam CT image reconstruction using GPU hardware, *Journal of X-Ray Science and Technology*, Vol. 16, pp. 225-234, ISSN 0895-3996

Yang, L.; Cai, Z., Wang G., Zhao, J. & Bai, E. W. (2009). Preliminary experimental results on controlled cardiac computed tomography: A phantom study, *Journal of X-Ray Science and Technology*, Vol. 17, pp. 175-187, ISSN 0895-3996

Yin, Z.; Khare, K. & De Man, B. (2009). Parametric boundary reconstruction algorithm for industrial CT metrology application, *Journal of X-Ray Science and Technology*, Vol. 17, pp. 115-133, ISSN 0895-3996

Zeng, K.; Bai, E.W. & Wang, Ge (2007). A Fast CT Reconstruction Scheme for a General Multi-Core PC, *Int J Biomed Imaging*, Published online 2007 July 9. doi: 10.1155/2007/29160, ISSN 1687-4196

Zeng, K.; Fajardo, L.L.; Kao, S., Franken, E. A., Park, Jeong M., Jing, Z., Bai, E.W. & Wang, G. (2008). An in vitro evaluation of cone-beam breast CT methods , *Journal of X-Ray Science and Technology*, Vol. 16, pp. 171-187, ISSN 0895-3996

Zhang, Y. & Ruola N. (2008). Investigation of image noise in cone-beam CT imaging due to photon counting statistics with the Feldkamp algorithm by computer simulations, *Journal of X-Ray Science and Technology*, Vol. 16, pp. 143-158, ISSN 0895-3996
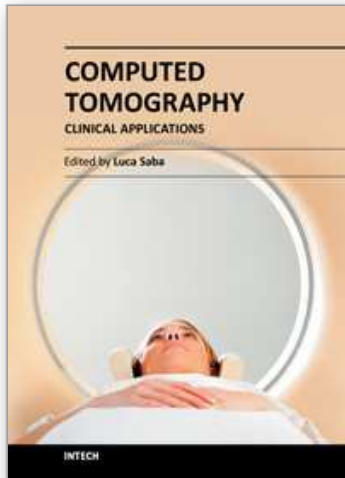
Computed Tomography - Clinical Applications

Edited by Dr. Luca Saba

Computed Tomography (CT), and in particular multi-detector-row computed tomography (MDCT), is a powerful non-invasive imaging tool with a number of advantages over the others non- invasive imaging techniques. CT has evolved into an indispensable imaging method in clinical routine. It was the first method to non-invasively acquire images of the inside of the human body that were not biased by superimposition of distinct anatomical structures. The first generation of CT scanners developed in the 1970s and numerous innovations have improved the utility and application field of the CT, such as the introduction of helical systems that allowed the development of the "volumetric CT" concept. In this book we want to explore the applications of CT from medical imaging to other fields like physics, archeology and computer aided diagnosis. Recently interesting technical, anthropomorphic, forensic and archeological as well as paleontological applications of computed tomography have been developed. These applications further strengthen the method as a generic diagnostic tool for non- destructive material testing and three-dimensional visualization beyond its medical use.

How to reference

In order to correctly reference this scholarly work, feel free to copy and paste the following:

Zhijun Cai, Er-Wei Bai and Ge Wang (2012). Dose Reduction on Computed Tomography Angiography Using Adaptive Control Techniques, Computed Tomography - Clinical Applications, Dr. Luca Saba (Ed.), ISBN: 978-953-307-378-1, InTech, Available from: http://www.intechopen.com/books/computed-tomography-clinical-applications/dose-reduction-on-computed-tomography-angiography-using-adaptive-control-techniques

INTECH
open science | open minds